

High-Charge, Multi-MeV Electron Bunches Accelerated in Moderate Laser-Plasma Interaction Regime

C.A. Cecchetti^{a,b}, S. Betti^{a,b}, A. Gamucci^{a,b}, A. Giulietti^{a,b}, D. Giulietti^{a,b,c}, P. Koester^{a,b,c}, L. Labate^{a,b}, N. Patak^{a,c}, F. Vittori^{b,c}, O. Ciricosta^{a,b,c}, L.A. Gizzi^{a,b}.

^a *Intense Laser Irradiation Laboratory-Istituto per i Processi Chimico-Fisici (IPCF) Consiglio Nazionale delle Ricerche (CNR), Pisa, 56124, Italy, (<http://ilil.ipcf.cnr.it>).*

^b *Istituto Nazionale di Fisica Nucleare (INFN), Sezione di Pisa.*

^c *Dipartimento di Fisica, Università di Pisa.*

Abstract. Experiments [1], and simulations[2] have shown that quasi-monoenergetic electron bunches can be accelerated from the background electron plasma population up to relativistic energies. Theoretical work [3] indicated that with a proper choice of laser, plasma, and injection parameters the acceleration of electron bunches with small energy spread and short bunch length can occur in moderate intensity regime. Here we present the results of an experiment on electron acceleration carried out at the IPCF-CNR's *Intense Laser Irradiation Laboratory* in Pisa [4], within a wide national collaboration led by INFN named PLASMONX [5]. High-charge, multi-MeV electron bunches were accelerated in moderated intensity regime by focusing the laser beam on a laminar gaseous target produced by a supersonic gas-jet. The laser-gas interaction was studied via interferometry, and Thomson scattering while the electron bunches were detected and characterised using a phosphor screen coupled with a magnetic spectrometer or a dosimetric detector. In some cases highly collimated electron bunches with moderate energy spread were observed, while the generation of high-charge, MeV energies electron bunches were obtained with high reproducibility for each gases tested.

Keywords: Electron acceleration, laser-plasma interaction, TW laser.

PACS: 52.38.-r; 52.38.Kd; 52.70.-m

INTRODUCTION

With the advent of the chirped pulse amplification technique a new generation of terawatt, compact laser systems have been created, and successfully used in many laboratories world-wide for the exploration of the laser-matter interaction in the ultra-short, ultra-intense domain. The wealth of new results thus obtained have generated new fields of research including X-ray sources, laser-driven acceleration, new scheme for the inertial fusion energy and warm dense matter physics. Among these new fields of research the exploitation of laser-driven particle acceleration caught the interest of the particle accelerator community for a new generation of accelerators. Laser WakeField Acceleration (LWFA) is among the most promising techniques for acceleration of electron bunches that takes advantage of the high electric fields supported in the plasma. In LWFA the electrons trapped in the plasma waves are accelerated up to phase velocity of the wave which can be very close to the speed of light. In this scenario the INFN-PLASMONX project exploits the coupling of an ultra-short laser pulses, 300 TW, Ti:Sa laser system FLAME (Frascati Laser for Acceleration and Multidisciplinary Experiments) with a 150 MeV SPARC [6] linear accelerator for developing a new generation of particle accelerator based on self- or externally injected electron bunches in plasma waves. Here we present the investigation of the electron bunches properties accelerated in moderated intensity regime 2 TW. Because of the laser system repetition rate (10 Hz) we took particular care on the development of the diagnostics involved in the experiment in view of the exploitation of laser-accelerated electron bunches for applications requiring high average bunch charge and moderate electron energy, including nuclear activation and Intra-Operatory Radiation Therapy (IORT) [7].

EXPERIMENTAL SET UP

The experiment carried out at the ICF-CNR's ILIL laboratory employed ~ 2 TW, $\lambda=800$ nm, 10 Hz laser pulse operating in chirped pulse amplification mode (CPA). The laser system can deliver two pulses at 67 fs, 130 mJ (CPA₁), and 10 mJ (CPA₂) respectively. The laser pulse containing the 90% of the front-end energy, CPA₂, is used for optical probing purposes, while the CPA₁ laser beam after amplification in a 6-pass amplifier, and compressed under vacuum, was focused with an $f/6$ off-axis parabola up to 6 μ m diameter focal spot onto the gas-jet target, as shown in fig.1. The gas-jet target was irradiated at full laser energy varying the gas backing pressure to change the value of the maximum density of the neutral gas.

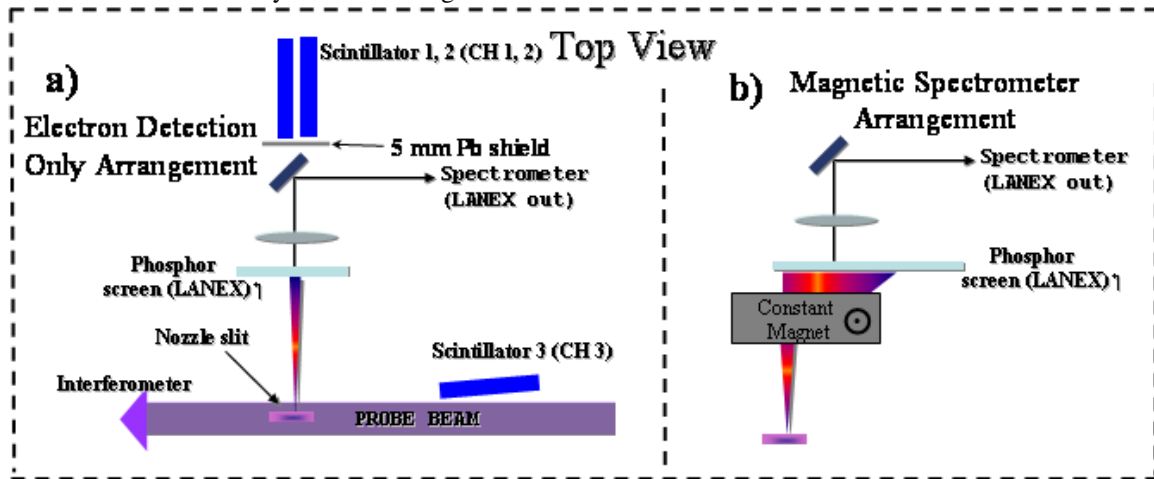


FIGURE 1. Schematic layout of the experimental setup: a) top view of the experiment in case of LANEX diagnostic without magnetic spectrometer for characterization of the electron bunches only (electrons detection configuration). The probe beam was used for the Nomarski modified Interferometry [8]. b) Top view of the LANEX diagnostic with magnetic spectrometer (electrons characterization configuration).

Targets characterised by different physical properties mainly related to the atomic number (He, and N₂) enabled us to explore the ionization properties under irradiation of ultra-short, intense laser pulses. The gas flows out of the slit in a laminar supersonic jet in order to produce steep interfaces between gas and vacuum, which is maintained at pressure of $\sim 10^{-4} \div 10^{-5}$ Torr. Nomarski modified interferometric diagnostic was set up perpendicularly to the CPA1 propagation axis to study and characterise its propagation through the gas and the plasma, as shown in Fig.1 a). A second group of diagnostics was fully devoted to the detection, and characterization of the electron bunches accelerated during the laser-gas interaction. Fig.1 shows the sketch of the experimental set-up, and the diagnostics arrangement in case of electron detection only, Fig.1a), and electron spectrum characterisation, Fig.1b). A set of 3 scintillators coupled to photomultipliers, and monitored with an oscilloscope detected the γ -rays produced via Bremsstrahlung by the electron within the walls of the vacuum chamber. As shown in fig.1 a), two scintillators shielded by a 5 mm layer of Pb (CH1 and CH2), were placed along the laser propagation axis and a third one (CH3), not shielded was placed perpendicularly to the mentioned direction. A 25 mm radius phosphor screens (LANEX) filtered by 25 μ m Al foil, was used for detection only and characterization of the electron bunches. In case of electron bunch characterization a magnetic spectrometer based upon permanent NeFeB magnets, generates a quasi-uniform magnetic field ($B_{\text{Max}} \sim 0.45$ T), placed in front of the phosphor screen spatially dispersing the electrons depending on their kinetic energy, see fig.1b). The other detector used for energy measurements was SHEEBA [9]. SHEEBA is an energy spectrometer consisting of sandwiched Radiochromic films [10], HD810 and MD55 in our case. Different types of RCF differ in the thickness of the active gel, and plastic substrates leading to different sensitivities to the action of the ionizing radiation, and dynamic range. Because their sensitive to the ionizing radiation SHEEBA first layer is always a Aluminum foil which act as a filter for optical and soft X-rays.

EXPERIMENTAL RESULTS

The experimental campaign was divided in two phases. In the first phase of the experiment the stability of the acceleration mechanism and the angular divergence of the electron bunches was studied using the set of three scintillators, and the phosphor screen LANEX. In the second phase of the experiment the magnetic spectrometer has

been aligned in front of the LANEX screen to detect the electron spectra. The SHEEBA detector was used to obtain independent spectrum, and angular distribution of electrons to be compared with the previous measurements. SHEEBA detector does not allow more than five consecutive acquisitions and cannot be used in a high repetition rate scenario and cannot be used simultaneously with the LANEX because both diagnostics need to be placed along the laser propagation axis.

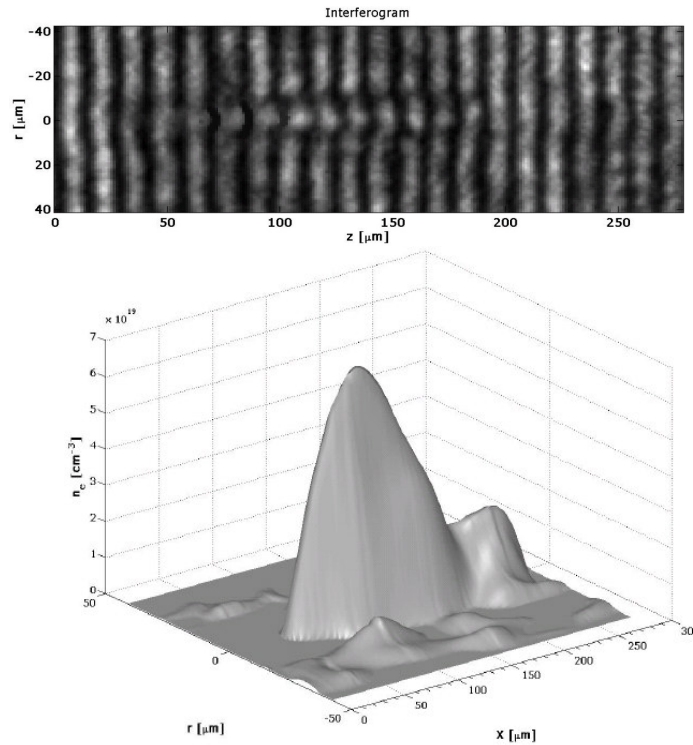


Figure 2. Interferometric image and its analysis. The shot was performed onto N2 gas @ 35 bar, with the focal plane 50 μm into the gasjet respect of the edge facing the incoming CPA1, and 500 μm from the nozzle.

Interferometry measurements were performed employing a Nomarski modified optical interferometer [11]. Optical interferometry was employed to retrieve information on the plasma density. The technique is based upon the dependence of the plasma refractive index on the electron density (1). As a consequence of the above relation a ray of an optical beam passing through the plasma acquires a phase shift (2) with respect to a ray which has traveled the same distance in vacuum.

$$\eta = \sqrt{1 - \frac{n_e}{n_c}} \simeq 1 - \frac{n_e}{2n_c} \quad (1) \quad \Delta\phi = -\frac{2\pi}{\lambda} \int_L [\eta(x, y, z) - 1] dx \simeq \frac{\pi}{\lambda n_c} \int_L n_e dx \quad (2)$$

By measuring the phase shift experienced by a laser beam probing the plasma, information about the electron density can therefore be obtained [11]. Fig.2 respectively show an interferogram, and its analysis, obtained in the early phase (~ -30 fs to CPA₁ peak) of the laser-gas interaction over a wide temporal range of 65 fs for a shot in which the diagnostics for electrons revealed the electron signal. The analysis of the electron density from the interferogram was performed using the code IACRE [12]. The density map thus obtained shows a maximum electron density of $7 \times 10^{19} \text{ cm}^{-3}$, and an approximately 200 μm long plasma channel, see fig.2. A fine temporal scan between the main pulse and the optical probe has been performed to monitor the pre-plasma eventually formed by the ASE or a pre-pulse. The interferograms acquired in this phase did not show pre-plasma formation.

In Fig.2 a), and b) are shown the typical image resulting from LANEX screen in two different shots, while fig.2 c) shows the signals acquired with the scintillators. In this phase of the experiment electron acceleration was always observed when the focal plane (depth of focus) was located in the proximity of the edge of the nozzle facing the incoming laser at ~ 0.6 mm from the top of the nozzle where the atom density can be estimate in the range of $1 \div 3 \times 10^{18} \text{ cm}^{-3}$ @ 50 bar back gas-jet pressure. A full scan in pressure has also been performed, revealing that at higher pressure more stable, but less collimated electron bunches were produced. In this scheme measurements of the electron bunches divergence have been performed showing a large divergence of approximately 20° FWHM in case

of N₂ gas, see fig.3a), while a much narrower angular distribution is found in the case of He gas which is of the order of 2° FWHM, shown in fig.3b).

In the case of the energy distribution measurements carried out using a magnetic spectrometer a Pb shield with a 0.5 mm slit width was placed in front of the magnets. Electrons propagating through the magnetic field are spatially dispersed on LANEX screen depending on their initial energy. A suitable algorithm was implemented in order to calibrate the imaged acquired with this system. The typical electron energy spectrum acquired during the experiment shown a clear peak located around 4-6 MeV, as shown in fig.4 a). The results obtained by the magnetic spectrometer were confirmed by the measurements carried out using the SHEEBA, see fig. 4b).

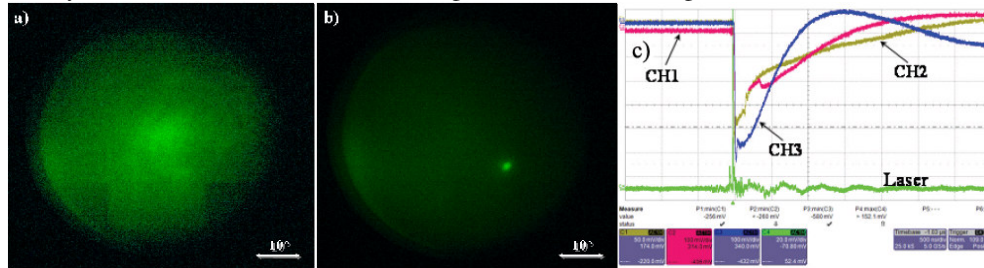


FIGURE 3. Typical outputs of LANEX in detection configuration. a) non-collimated laser-accelerated electrons in case of N₂ gas @ 50 bar. b) collimated, laser-accelerated electron bunch in case of He gas @ 50 bar. c) Output signals of the scintillators as labeled in fig.1, and diode signal generated by the CPA1 beam (trigger).

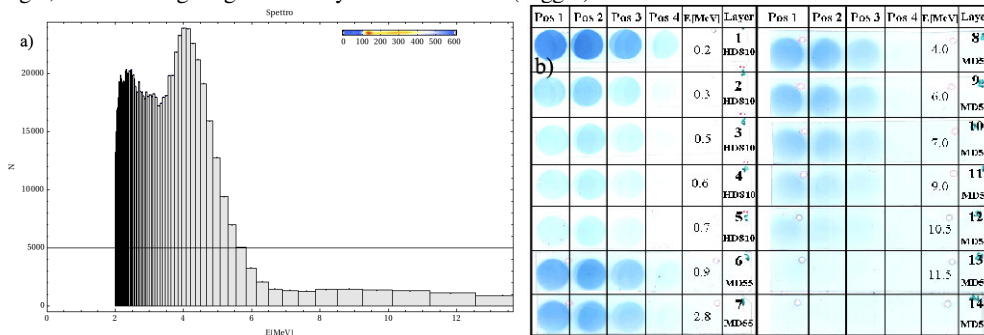


FIGURE 4. a) Typical calibrated electron spectrum with quasi-monoenergetic peak around 4-5 MeV. On the up-right corner of the LANEX image of a typical dispersion stripe with structure toward high energies. b) SheeBA output. Columns from Pos1 to Pos4 represent the positions, the column “E” the electron energy in MeV, and the last one the layer and type of radiochromic films. In case of Pos1, 2, and 3 a series of 21, 10, and 5 consecutive shots have been taken before to move toward the next position. Position 4 represents one shot only.

The experiment provided relevant for future applications as Intra-Operatory Radio-Therapy (IORT), thanks to the high charge of our bunches and to low operational costs implied by our experimental configuration.

This work was supported by the INFN Project PLASMONX, and by the MIUR funded FIRB-SPARX project and by the MIUR-PRIN project. We acknowledge the support of the CINECA computing center for the 3D simulations.

REFERENCES

1. J. Faure, et al., *Nature (London)* **431**, 541 (2004).
2. A. Pukov, J. Meyer-ter-Nehn, *Appl. Phys. B*, **74**, 355 (2002).
3. R.F. Hubbard, et al., *IEEE Trans. Plasma Sci.*, **33**, 712 (2005).
4. L.A.Gizzi. Laser-plasma acceleration: First experimental results from the plasmon-x project. In World Scientific, editor, Channeling 2008, Science and Culture Series, 2009.
5. L.A. Gizzi, et al., *Europ. Phys. Journal - Special Topics*, **175**, 3-10 (2009).
6. D. Alesini, et al., *Nucl. Instr. and Meth. A*, 507, 345 (2003).
7. D A. Giulietti, et al., *Phys. Rev. Lett.*, **101**, 105002 (2008).
8. R. Benattar, C. Popovics, and R. Sigel, *Rev. Sci. Instr.*, **50**, n.12, 1583 (1979).
9. M. Galimberti, et al., *Rev. Scien. Instr.*, **76**, 053303 (2005).
10. Z. Cai, et al., *Phys. in Med. and Biol.*, 48, 4111 (2003).
11. L.A.Gizzi, et al., *Phys.Rev.E*, **49**, 6. 5628 (1994).
12. P. Tomassini, et al., *Appl.Opt.*, **40**, 35, 6561(2001).